Available online at www.sciencedirect.com
SCIENCE DIRECT®
PERGAMON
International Journal of Rock Mechanics & Mining Sciences 40 (2003) 609–631
International Journal of Rock Mechanics and Mining Sciences
www.elsevier.com/locate/ijrmms

Stability assessment of the Three-Gorges Dam foundation, China, using physical and numerical modeling—Part I: physical model tests

Jian Liu[a,b,*], Xia-Ting Feng[a], Xiu-Li Ding[b], Jie Zhang[b], Deng-Ming Yue[b]

[a] *Institute of Rock and Soil Mechanics, Chinese Academy of Sciences, Xiaohongshan, Wuhan, Hubei 430071, China*
[b] *Yangtze River Scientific Research Institute, Wuhan 430019, China*

Accepted 31 March 2003

Abstract

Foundation stability is one of the most important factors influencing the safety of a concrete dam and has been one of the key technical problems in the design of the Three-Gorges Project. The major difficulties lie in two facts. The first one is that the dam foundation consists of rock blocks, with joints and so-called 'rock bridges' and the gently dipping joints play a critical role in the foundation stability against sliding. The second one is that, even in the regions where the gently dipping fractures are most developed, there are no through-going sliding paths in the rock mass due to the existence of the rock bridges; so the dam could slide only if some of the rock bridges fail, so as to create at least one through-going sliding path. To date, due to unavoidable shortcomings in physical and numerical modeling techniques, there is not a single satisfactory method to solve the problem completely. For this reason, the integration of multiple methods was adopted in this study and proved to be an effective and reliable approach.

This Part I paper describes work based on the results of geological investigations and mechanical tests, relating to the geological and geomechanical models of the Three-Gorges Dam, and then a systematic study procedure was developed to carry out the stability assessment project. Then, 2D and 3D physical model tests for some critical dam sections were performed. In the physical tests, based on similarity theory, various testing materials were selected to simulate the rock, concrete, fracture and rock bridge. The loading and boundary conditions were also modeled to meet the similarity requirements. The failure mechanism was derived through a progressive overloading that simulated the upstream hydrostatic pressure applied to the dam, and the factor of safety was defined as the ratio between the maximum external load inducing the start of sliding instability of the dam foundation and the upstream hydrostatic load. The experimental results indicated that the stability of the Three-Gorges Dam foundation satisfies the safety requirements. Nevertheless, further discussions demonstrated that because of the incomplete definition of factor of safety adopted in the physical model tests, it is also essential to study the stability of the Three-Gorges Dam foundation using numerical modeling, which will be presented in the companion Part II paper.

Keywords: Dam foundation; Stability assessment; Physical model test; Gently dipping joint; Rock bridge; Three-Gorges Dam

1. Introduction

Foundation stability is one of the most important factors influencing safety of a dam. Instability of a dam generally results from pre-existing geological features in the foundation, such as faults, joints, soft rocks and solution channels, etc. Therefore, for a dam foundation, stability analyses and assessment are essential and form a critical part of the safety assessment.

The Three-Gorges water conservancy complex located about half way along the Yangtze River is the largest multipurpose water conservancy project ever built in China, indeed in the world (Fig. 1). The Three-Gorges Dam is one of the three main parts of this project (the others are the power houses and navigation facilities). It is a concrete gravity dam with a maximum height of 185 m and is designed to withstand a normal pool level of 175 m. According to the general layout of the dam (Figs. 2–4), 23 spillway-dam sections are

*Corresponding author. Institute of Rock and Soil Mechanics, Chinese Academy of Sciences, Wuhan, Hubei 430071, China.
Tel.: +86-27-871-97913; fax: +86-27-871-97386.
E-mail address: jliu@dell.whrsm.ac.cn (J. Liu).

1365-1609/03/$ - see front matter © 2003 Elsevier Ltd. All rights reserved.
doi:10.1016/S1365-1609(03)00055-8

Nomenclature

L_p	geometrical parameter of the prototype
σ_p	stress of the prototype
ε_p	strain of the prototype
δ_p	displacement of the prototype
E_p	deformation modulus of the prototype
v_p	Poisson's ratio of the prototype
X_p	volume force of the prototype
ρ_p	density of the prototype
f_p	friction coefficient of the prototype
c_p	cohesion of the prototype
R_p	compressive strength of the prototype
$\bar{\sigma}_p$	boundary stress of the prototype
L_m	geometrical parameter of the model
σ_m	stress of the model
ε_m	strain of the model
δ_m	displacement of the model
E_m	deformation modulus of the model
v_m	Poisson's ratio of the model
X_m	volume force of the model
ρ_m	density of the model
f_m	friction coefficient of the model
c_m	cohesion of the model
R_m	compressive strength of the model
$\bar{\sigma}_m$	boundary stress of the model
C_L	similarity constants for geometry
C_σ	similarity constants for stress
C_ε	similarity constants for strain
C_δ	similarity constants for displacement
C_E	similarity constants for deformation modulus
C_v	similarity constants for Poisson's ratio
C_X	similarity constants for volume force
C_ρ	similarity constants for density
C_f	similarity constants for friction coefficient
C_c	similarity constants for cohesion
C_R	similarity constants for compressive strength
$C_{\bar{\sigma}}$	similarity constants for boundary stresses

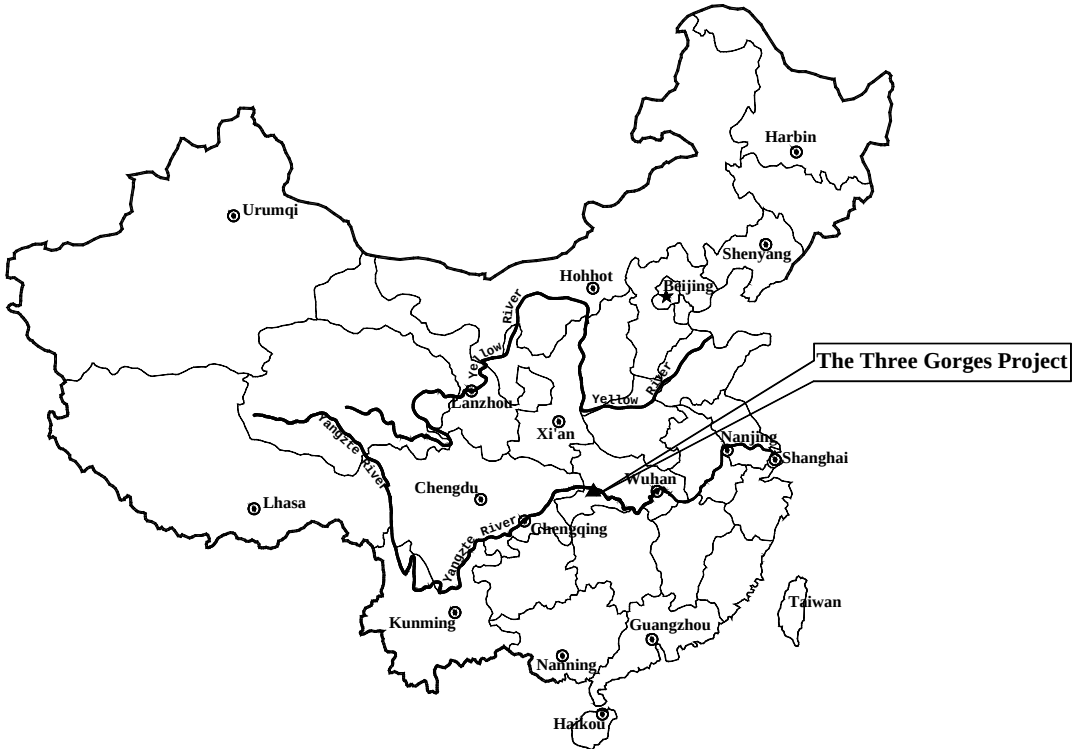

Fig. 1. Location of the Three-Gorges Project in China.

located in the middle of the riverbed with a total length of 483 m, 26 powerhouse-dam sections are situated at the two sides of the spillway dam and have a total length of 1228 m. Along the foundation line, the dam sections are built on different ground levels, low on the river bottom and high on the riverbank. Detailed geological investigations show that although the dam foundation mainly comprises plagioclase granite that is intact, homogeneous, of low permeability and high strength, there also exist weathered zones, faults and joints in the rock mass. In particular, gently dipping joints are well developed locally. When the project is finished and runs at the normal pool level, the resulting reservoir will extend nearly 600 km upstream and have a total storage

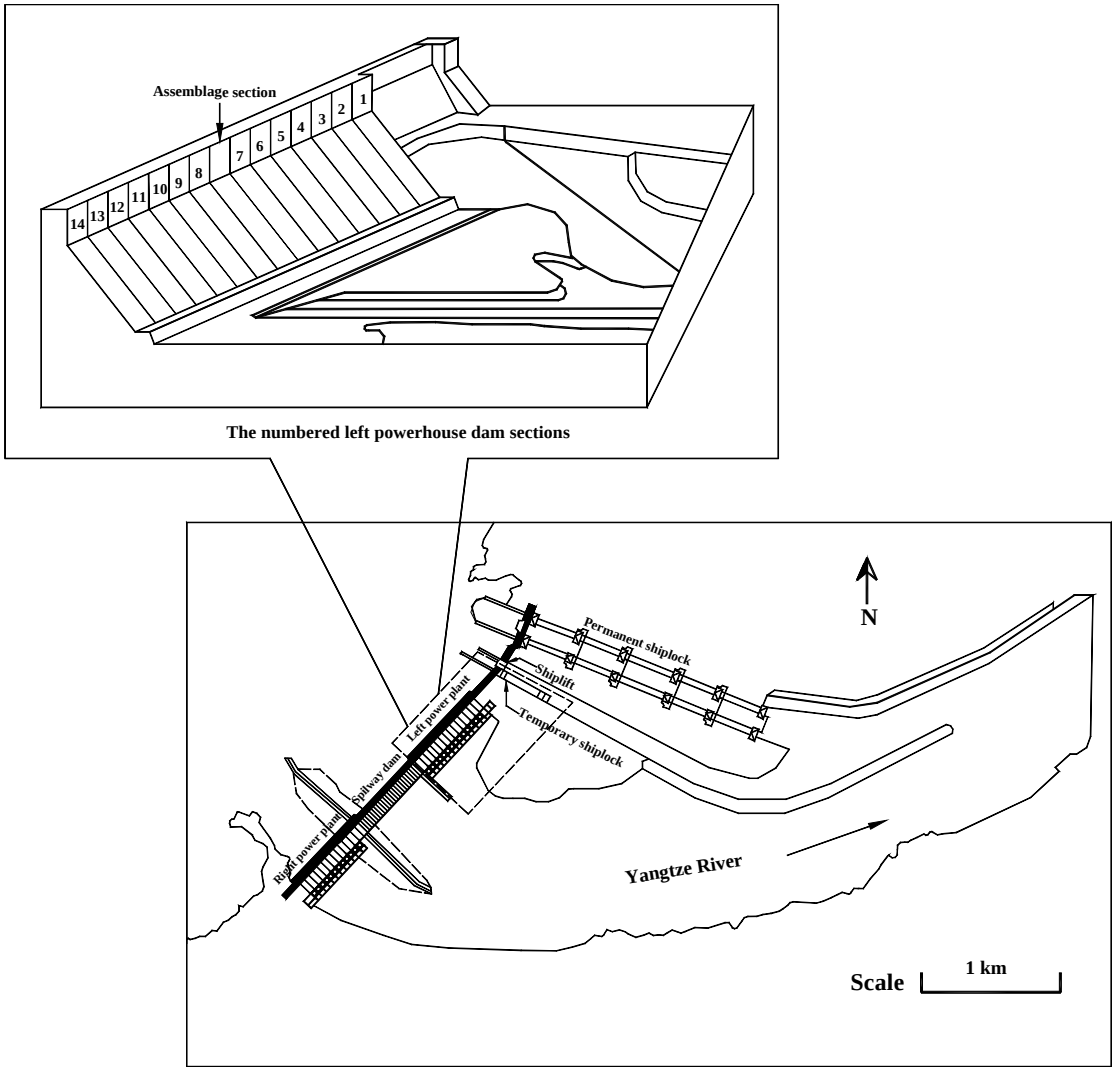

Fig. 2. Layout of the Three-Gorges Project and the numbered left powerhouse-dam sections.

Fig. 3. Upstream view of the Three-Gorges Project under construction.

capacity of 39.3 billion cubic meters, which is of extreme importance to the safety of the dam.

During the past decades, the Yangtze Water Resources Commission (CWRC), with the collaboration of the Chinese Academy of Science, the Ministry of Geology, and a number of universities and institutes of China, carried out extensive geological investigations, field and laboratory testing of the rock and soil properties related to the Three-Gorges Dam. This research work has been thorough and systematic, and

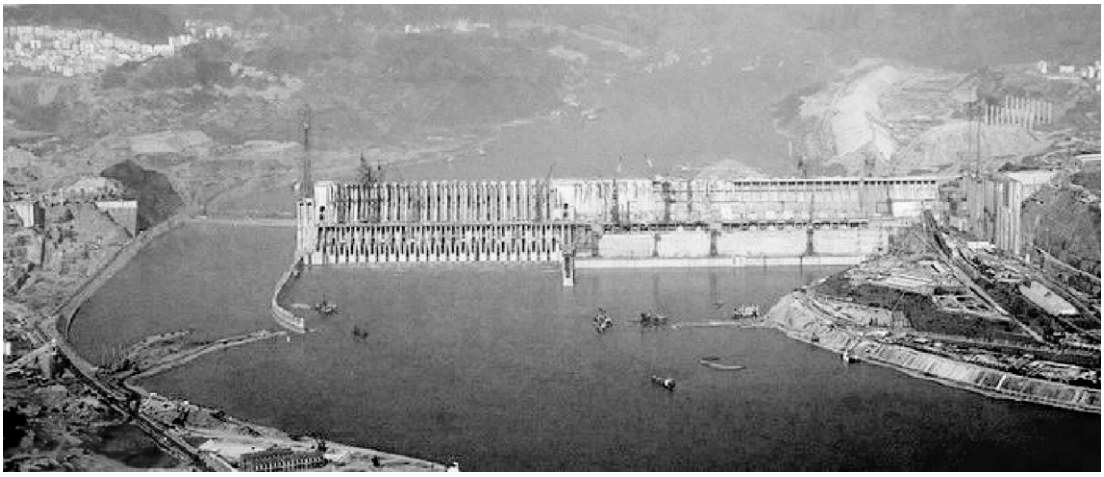

Fig. 4. Downstream view of the Three-Gorges Project under construction.

provided sufficient data for the stability analyses [1]. However, to study and assess the stability of the Three-Gorges Dam foundation, the following questions have to be addressed:

- The dam foundation mainly consists of rock blocks, various faults, fractures, joints and so-called 'rock bridges' (defined as the intact rock between the ends of sub-parallel fractures). Most of the faults and joints have a steep dip angle, but there are gently downstream-dipping joints that are actually the most important factors influencing the stability of the dam. On the other hand, even in the regions where the gently dipping fractures are most developed, no deterministic and through-going sliding paths in the rock mass exist due to the presence of the rock bridges. Thus, the dam could slide only if some of the rock bridges fail, so as to create at least one through-going sliding path. Therefore, in the stability analyses, taking account of the effects of the rock bridges becomes one of the key issues.
- Generally, two types of modeling approaches are adopted in stability analyses: physical model test and numerical modeling, including limit equilibrium method (LEM), finite element method (FEM), distinct element method (DEM) and discontinuous deformation analyses (DDA). The LEM has the advantage of simplicity and can provide a simple index of relative stability in the form of the factor of safety. Nevertheless, it considers only force and moment equilibria; deformations and material constitutive relations are not accounted for [2,3]. The FEM considers deformations and material constitutive relations and provides more information about distributions of stresses, deformations and possible failure or damage zones, but has limited capacity in identifying explicitly the critical state of sliding and failure of the dam. The DEM/DDA approach is based on dynamic motion of rock blocks that can also be deformable [4]. One of the strengths of the DEM/DDA method is that, as time progresses, the blocks are allowed to move and deform, so that the mode of failure becomes apparent [2]. However, although this approach is specifically suited for carrying out discontinuum analyses in rock mass, it suffers some practical limitations since numerical stability and convergence depend on the proper selection of time steps and damping parameters [5]. More importantly, the discrete numerical approaches, like DDA and DEM, needs detailed fracture system geometry that is often not readily available [6], and they are not efficient for problems with non-persistent fracture systems and rock bridges. The physical model tests that use simulated materials based on the theory of similarity can provide a direct perceptional methodology [7,8] and can automatically simulate the system performance of both dam and its foundation from elastic and elastic–plastic deformation to failure during the loading process [9–11]. However, such modeling costs much more and offers a limited amount of experimental output. Due to these shortcomings in each of the methods stated above, there is no single satisfactory method to fully solve the problem and so the integration of multiple methods became necessary. The main concern is how to properly treat the differences among their results and reduce the impacts of their shortcomings in the assessment of the stability of the dam.
- The Three-Gorges Dam consists of more than 50 dam sections with transverse concrete joints connecting them. The stability conditions are different between the sections because of the differences in the local geological conditions. Detailed study of each dam section is too costly and may not be necessary. Hence, picking out the representative

sections for stability studies, using the knowledge from the geological investigation and conceptualization [12–14], is a critical process.

A systematic study procedure was established to carry out this stability assessment project. Based on the results of geological investigations and mechanical tests of the rock mass, the geological and geomechanical models of the Three-Gorges Dam foundation were firstly established and a study procedure for the stability assessment was provided. Then, using the same geomechanical model, 2D and 3D physical model tests for some critical dam sections were performed. In the physical model tests, various testing materials were selected to simulate the rock, concrete, fracture and rock bridge. The prototype load and boundary conditions were also modeled according to similarity theory. During the testing process, the displacements at some important positions of the dam structure and foundation were monitored. The failure mechanism of the dam foundation was derived through a progressive overloading that simulated the upstream hydrostatic water pressure, and the factor of safety was defined as the ratio between the maximum external load inducing the start of sliding instability of the dam foundation and the upstream hydrostatic load applied to the dam. The comparisons between the results of 2D and 3D physical model tests were conducted.

This study mainly concerns the following aspects: (1) establishment of the geomechanical model of the dam foundation; (2) physical model tests; (3) numerical modeling; (4) comprehensive stability assessments based on modeling results; (5) additional treatment and reinforcement design. Part I of this paper describes the characterization and conceptualization of the geomechanical conditions of the foundation, and physical model tests. The Part II companion paper presents the numerical modeling, comprehensive assessment, reinforcement measures, and the overall conclusions.

2. Site geology and mechanical properties of the rock mass

2.1. Site geology

For identifying the geological setting at the dam site, various exploration techniques and methods were adopted, including conventional techniques (such as geological mapping, borehole drilling, adit, shaft exploration, etc.), geophysical prospecting (such as acoustic emission, remote sensing techniques, seismic reflection, seismic refraction and electromagnetic wave techniques), physical–chemical analysis and microstructural analysis, etc. The investigations covered basically all the geologic aspects, including regional geology, regional geomorphology, quaternary geology and hydrogeology at the dam site [1,15]. This provides a sound and adequate basis for the stability assessment.

The investigations show that the foundation rock mainly comprises plagioclase granite which is intact, homogeneous and of high strength. According to the degree of weathering, the typical weathered profile may be divided into four zones (Figs. 5 and 6): completely weathered, highly weathered, moderately weathered, and slightly weathered zones. The moderately weathered zone can be further subdivided into an upper part and a lower part. The total thickness of the first three weathered zones varies gradually from the ridge at riverbank (40–42 m) to floodplain (17–20 m) and to low-water riverbed (11 m), while the thickness of the slightly weathered zone is absent or very thin in the riverbed. The dam foundation is located on the lower part of the moderately weathered zone or on the top of the slightly weathered zone.

Major faults and their dip angles at the dam site are illustrated in Fig. 7. There are 886 faults identified with mostly steep dip angles. The statistical analysis demonstrates that 90% of them have lengths of less than 300 m and widths of less than 1 m. In accordance with their strike and persistence, these faults can be classified into four groups.

- The first group has trends NNW of 330–355°, with dip angles of 60–80°. They constitute 49% of the total fault population.
- The second group has NNE strikes of 5–30° with dip angles of 55–75°, constituting 27% of the total population.

Fig. 5. Borehole core of the granite rock in the dam site (core diameter is 800 mm).

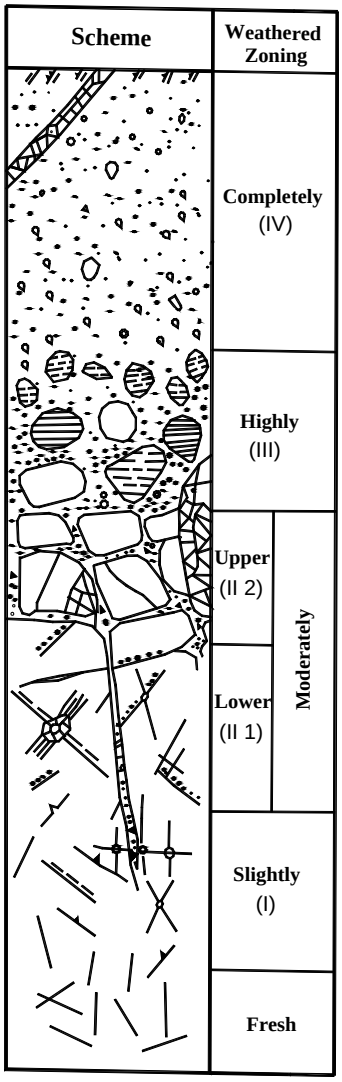

Fig. 6. Profile of typical weathering of the granite.

- The third group has NE–NEE strikes of 40–70° with dip angles of 65–85°, constituting 16% of the total population.
- The fourth group has trends of NWW–EW of 270–300° with dip angles of 60–85°, constituting 8% of the total population.

Most of the faults have well-cemented tectonite. Soft tectonite is seen in the latter two groups only, with such faults being few in number and small in size.

Joints are well developed in the rock mass. Statistically, steeply dipping joints (with dip angles of more than 60°) are dominant and take up more than 70% in the total joint population. Respectively, moderately dipping joints (with dip angles of 30–60°) and gently dipping joints (with dip angles of less than 30°) take up 10% and 13% of the total population, respectively. Fig. 8 illustrates the pole density contour of the gently dipping joints investigated in the foundation of the left powerhouse-dam sections of the Three-Gorges Dam. Similar to the features of the faults, the steeply and moderately dipping joints may also be classified into four sets (namely, NNW, NNE, NEE and NWW sets) and each group basically has the same strikes and dip angles as those of the corresponding fault groups.

The gently dipping joints have been studied more in detail because of the fact that most of them dip downstream with a low angle and may possibly create potential sliding surfaces in the foundation. They were categorized into two types, namely long gently dipping joints (with a length of more than 10 m) and short gently dipping joints (with a length of less than 10 m). Table 1 lists the geological characteristics of long gently dipping joints, which mostly have hard surfaces with epidotic or feldspathic fillings. The short gently dipping joints

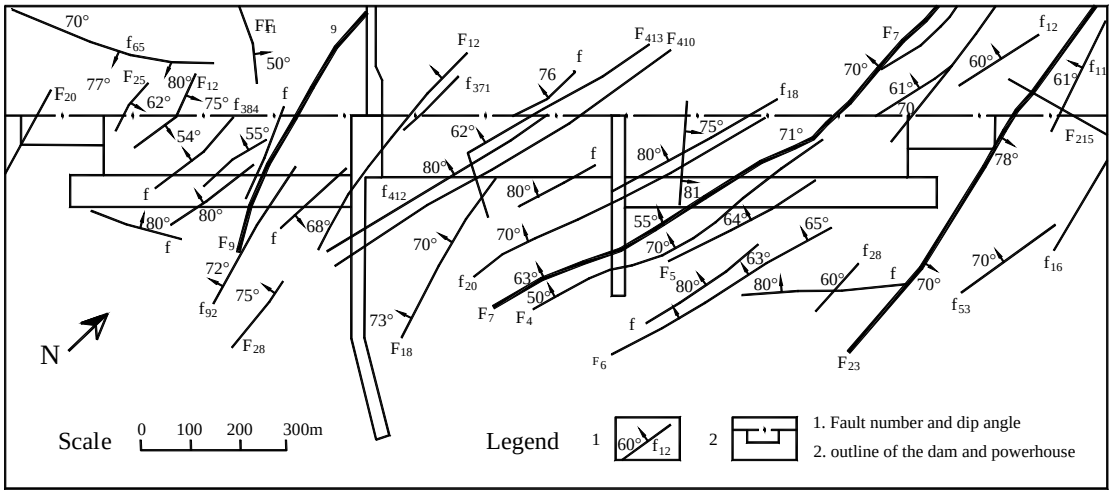

Fig. 7. Plan of the distribution of the dominant faults in the foundation of the Three-Gorges Dam.

constitute more than 90% of the total population of these two joint groups. Considering that the gently dipping joints play an important role in the foundation stability, their distribution was divided into three kinds of regions with different densities along the vertical direction in the boreholes. The statistical analysis showed that, in the dam foundation, the average density of short and long gently dipping joints is 0.24 and $0.018\,m^{-1}$, respectively [15–17]. Fig. 9 depicts these regions with the different densities. They are:

- *relative developed region* (I): long and short gently dipping joints are both well developed, with linear densities more than 0.024 and $0.31\,m^{-1}$, respectively;
- *slightly developed region* (II): either the density of long gently dipping joints is more than $0.024\,m^{-1}$, or, the density of short gently dipping joints is more than $0.31\,m^{-1}$;
- *poor developed region* (III): the densities of both long and short gently dipping joints are, respectively, less than 0.024 and $0.31\,m^{-1}$.

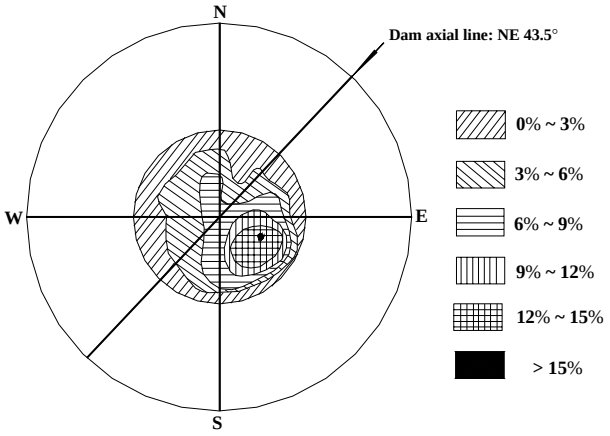

Fig. 8. Pole density contour plot of the gently dipping joints investigated in the foundation of the left powerhouse-dam sections of the Three-Gorges Dam.

2.2. Mechanical properties of the rock mass

To define the physical and mechanical properties of the rocks and fractures, both field and laboratory tests were performed [18]. In addition, the deformation behavior of the rock mass was acquired by means of plate bearing tests; the shear strengths of the rock and fractures were tested through in situ and laboratory shear tests; the failure behavior of the rock mass was obtained from triaxial tests [15–23]. The properties of

Table 1
Characteristics of the long gentle dipping joint sets in the Three-Gorges Dam foundation

Joint set	Dip direction	Dip	Developed level	Characteristics of joint surfaces
1	90–120°	15–30°	Relatively developed	The joint surfaces are planar rough or undulating rough with joint fillings of epidote
2	50–80°	10–30°	Slightly developed	The joint surfaces are planar rough or undulating rough with joint fillings of epidote or feldspathic minerals
3	170–190°	10–30°	Poorly developed	The joint surfaces are undulating rough, without or with joint fillings of epidote
4	130–150°	10–30°	Poorly developed	The joint surfaces are planar rough without joint fillings

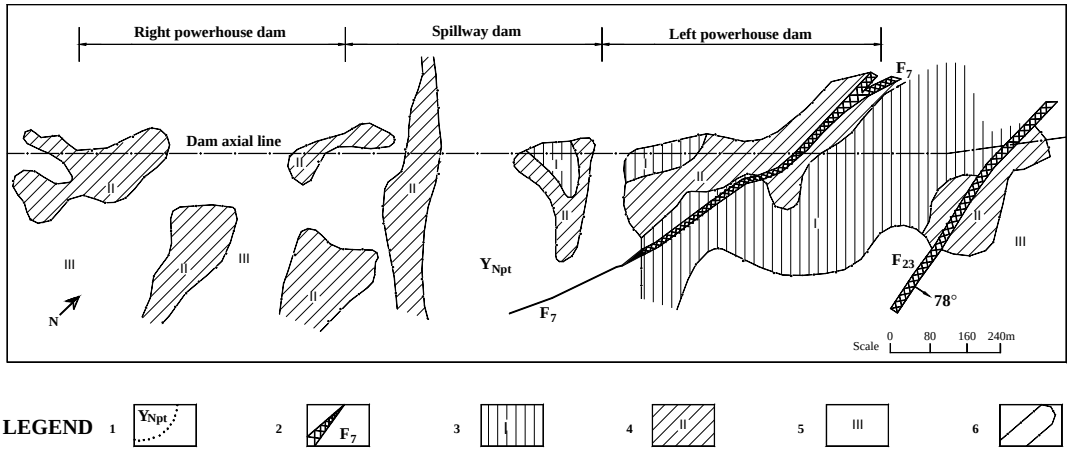

Fig. 9. Plan of the developed regions of gently dipping joints (with different densities) in the Three-Gorges Dam foundation.

Table 2
Geotechnical properties of the plagioclase granite in the Three-Gorges Dam foundation

Degree of weathering	Structural types of rock mass	Compressive strength (wet) (MPa)	Density (kN/m^3)	Deformation modulus (GPa)	Poisson's ratio	Friction angle	Cohesion (MPa)
Fresh	Blocky	90–110	27.0	35–45	0.20	59.6°	2.0–2.2
Slightly weathered	Sub-blocky	85–100	27.0	30–40	0.22	56.3°	1.6–1.8
	Inlaid structure	85–100	26.8	20–30	0.22	52.5°	1.4–1.6
Moderately weathered (lower part)	Blocky	75–80	26.8	20–30	0.22	56.3°	1.6–1.8
	Sub-blocky	75–80	26.8	15–20	0.23	52.5°	1.4
	Inlaid structure	70–75	26.5	10–15	0.25	50.3°	1.0
Moderately weathered (upper part)	Blocky	40–70	26.8	5–20	0.25	50.3°	1.0
	Fractured	15–20	25.5	1–5	0.27	—	—

Table 3
Mechanical parameters of structural planes in the plagioclase granite

Types of structural planes	Friction angle	Cohesion (MPa)
Planar smooth	31°	0.13
Planar rough	37°	0.3
Combination of the above two types	35°	0.2
Rough	42°	0.5
Extreme rough	45°	0.6

plagioclase granites and structural planes are listed in Tables 2 and 3, respectively.

3. Model conceptualization and study procedure for stability analyses

Due to the complexity of the natural geological conditions and variability of mechanical properties of rock masses, it is difficult to accurately and fully simulate the geological conditions and the mechanical properties of the rock mass—even with the costly and time-consuming work of extensive in situ and laboratory characterization as carried out for the Three-Gorges Project. Hence, it is recognized that rational simplification and conceptualization of both geological conditions and mechanical properties of rock masses are necessary for physical model tests and numerical modeling [12–14].

The conceptualization process considered the following steps: (1) careful verification of the underlying geological conditions, such as rocks, discontinuities and their distributions; (2) determination of the mechanical parameter values of rocks and discontinuities; (3) pre-analysis of possible sliding mechanisms and identification of all the potential sliding paths; (4) on account of the discrepancies unavoidably occurred during the test period, a safety margin for errors has to be considered and reserved; (5) based on all the above steps, choosing the most important and representative dam sections to be simulated. Meanwhile, to pre-analyze the potential sliding paths and possible failure mechanisms, the following aspects have been taken into account: (i) spatial geometrical characteristics of each fracture explored, such as inclination and dip angle; (ii) combinative spatial geometrical properties of fracture system (such as connectivity) by which potential sliding paths could be formed; (iii) relative distance between fractures and the upper concrete structure; (iv) mechanical properties of the intact rock and fractures.

Based on the above rationalization, the geological conceptualization of the Three-Gorges Dam foundation was carried out in the following sequence.

(1) Because the weak weathered zones would be mostly excavated and the foundation mainly consists of plagioclase granite that is intact, homogeneous and of high strength, the major factor influencing the foundation stability would come from the pre-existing discontinuities. However, among these discontinuities, the faults mostly have steep dip angles (as depicted in Fig. 7), thin thickness, and well-cemented tectonite, so they would not play important roles in the foundation stability.
(2) Most of the joint sets have steep or moderate dipping angles as those of the fault groups, and would also play a less important role in the foundation stability.

(3) The gently dipping joint sets that have low angles and dip downstream would be the most important factor governing the foundation stability. Among them, the long gently dipping joints, especially those that dip downstream and have acute angles between their strikes and the dam axial line, are the most likely ones to create sliding paths [15–17]. Therefore, the potential sliding paths could be assumed according to the following reasons: (i) the assumption of sliding paths can be based on gently dipping joints, geological profiles of the foundation and dam structures. (ii) the assumed potential sliding path must consider the combined effects of long gently dipping joints, rock bridges and short gently dipping joints, which are produced by projecting short gently dipping joints on the assumed sliding path. (iii) the assumed sliding paths could be linear, curved or stepped. The mechanical properties of the long and short gently dipping joints are assumed to be the same.

(4) Gently dipping joints are concentrated in the foundation of no. 1–5 left powerhouse-dam sections (as shown in Fig. 9, for the locations of these sections see Fig. 2), with the long gently dipping joints having a dominant strike of 28°, inclination of 118° and dip angles of 25–27°. In addition, an exposed steep rock slope (with a temporary height of 67.8 m and permanent height of 39.0 m) will be excavated on the foundation behind the dam and dipping downstream. Its downstream free face would lead to less resistance against potential sliding. From the above reasoning, it is concluded that the sliding-resistant capacities of no. 1–5 left powerhouse-dam sections are the poorest of the dam foundation. Our studies are therefore concentrated on the stability of no. 1–5 left powerhouse-dam sections.

(5) Further detailed investigations showed that in the foundation of the no. 3 left powerhouse-dam section, both the average linear fracture density (cf. Table 4) and the potential of the sliding path formation (Figs. 10) of the gently dipping joints are the greatest. Figs. 11 and 12 show the section of geological sketch and Stereographic projection of

Table 4
Comparison of the average linear densities of long gentle dipping joints distributed in the foundations of no. 1–5 left powerhouse dam sections

	No. 1 section	No. 2 section	No. 3 section	No. 4 section	No. 5 section
average linear densities (number/m)	Less than 0.078	0.071	0.121	0.078	Less than 0.071

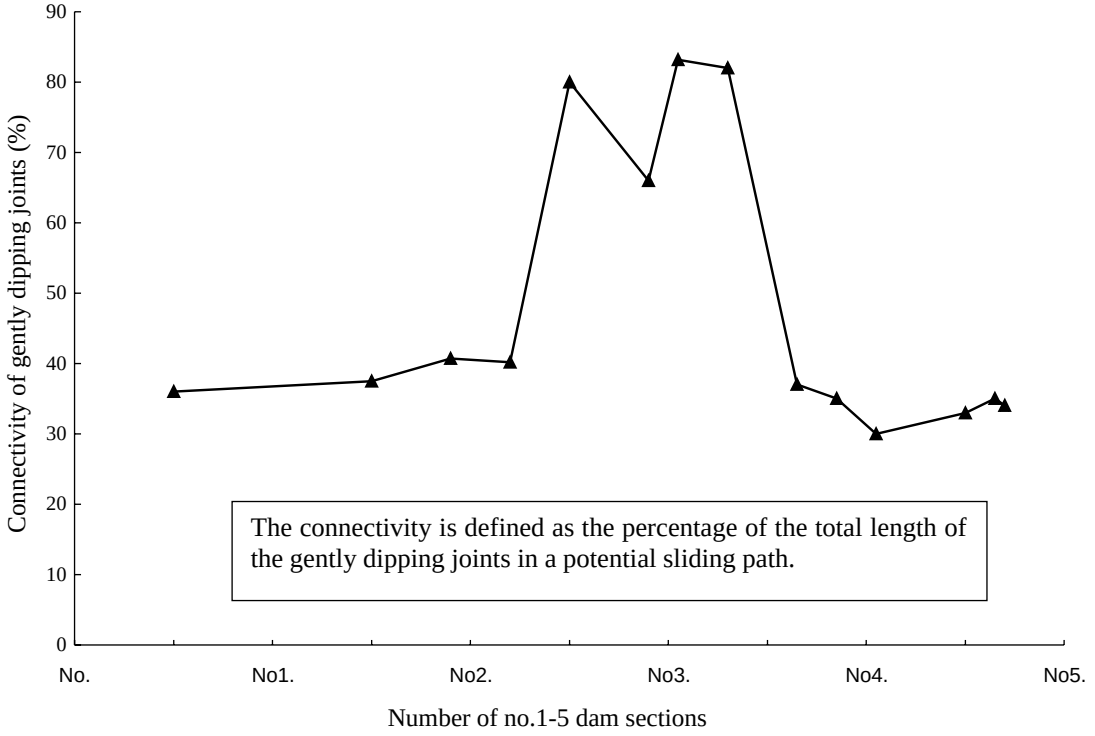

Fig. 10. Connectivity distribution of the gently dipping joints of main potential sliding paths in the foundation of no. 1–5 powerhouse-dam sections.

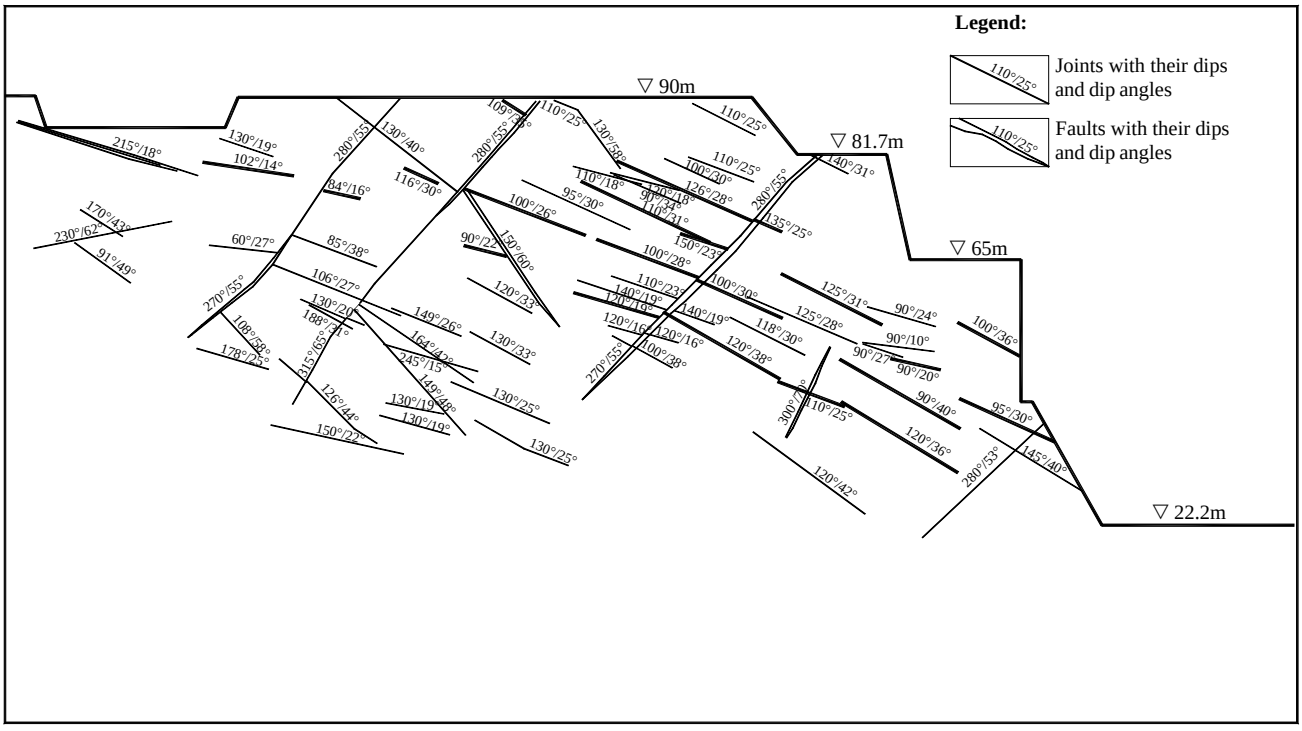

Fig. 11. Geological section sketch of no. 2 powerhouse-dam section of the Three-Gorges Dam.

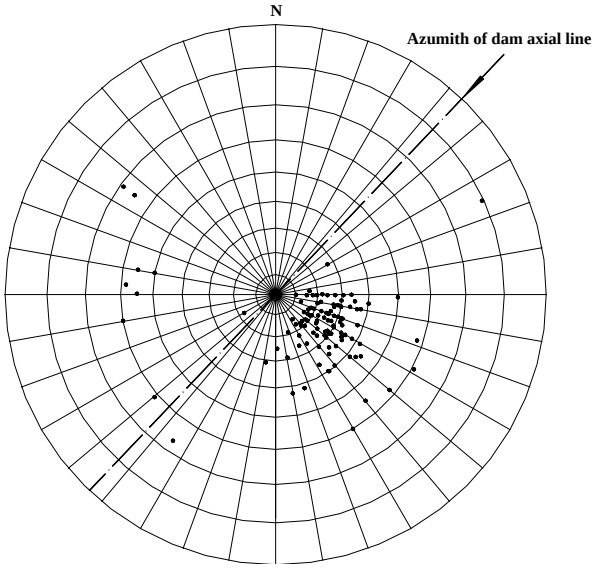

Fig. 12. Stereographic projection of the joints in the foundation of no. 3 powerhouse-dam section of the Three-Gorges Dam.

the joints in the foundation of no. 3 powerhouse-dam section. Therefore, the no. 3 left powerhouse-dam section is most likely the most unstable of these five dam sections, and should be chosen as the basis of the model establishment.

The geological model of no. 3 powerhouse-dam section is illustrated in Fig. 13. For investigating the constraint effects on the stability of this section provided by the foundations of the adjacent no. 2 and no. 4 powerhouse-dam sections, the stability of all these three dam sections needs to be studied. The geological models of no. 2 and no. 4 sections are given in Figs. 14 and 15, respectively. The characteristics of the main assumed sliding paths in the above three geological models are, respectively, listed in Tables 5–7.

As for the mechanical parameters of the rock and fractures, statistic analysis, fuzzy selection and optimized rate of oblique method were applied [15–23]. On the basis of the results acquired by these methods, the mechanical parameters were determined for the stability analyses as listed in Table 8.

Summarizing the process of conceptualization and parameterization as aforementioned, the study procedure for the stability assessment of the Three-Gorges Dam foundation is given by the flowchart shown in Fig. 16.

4. Physical model tests: similarity theory and experimental method

Physical model tests are the laboratory simulation of natural processes at a proportionally reduced scale. When the processes to be studied are so complex that a mathematical representation is not easy, physical models are often necessary to identify the key mechanisms, and are an instrument for validation and calibration of numerical models [24,25].

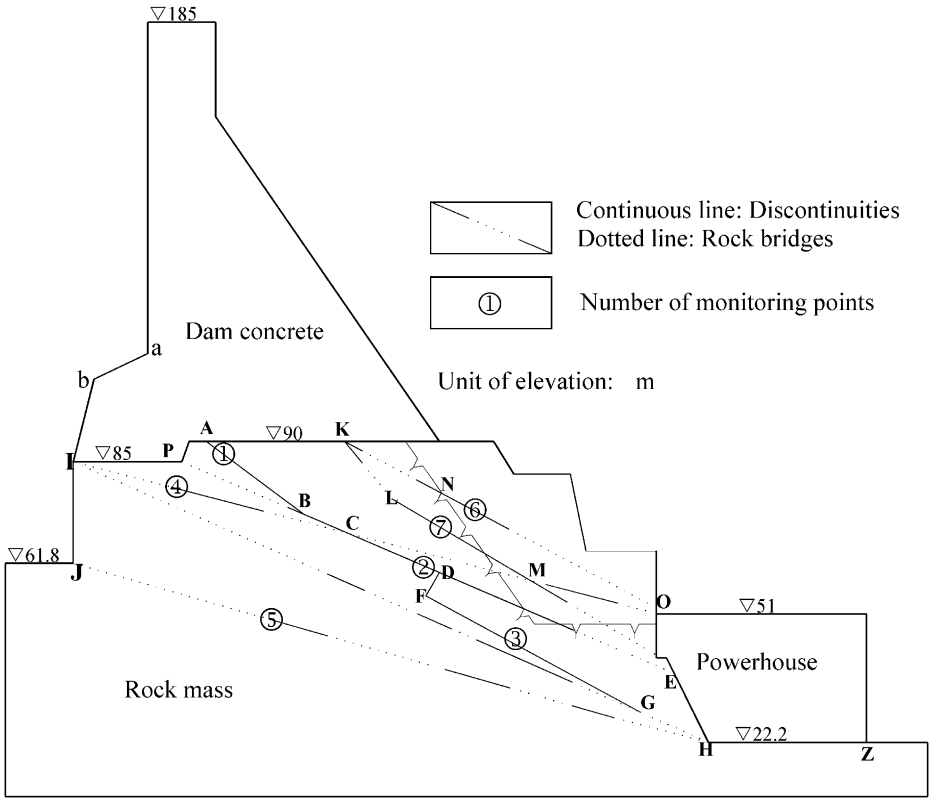

Fig. 13. Geological model of no. 3 left powerhouse-dam section of the Three-Gorges Dam.

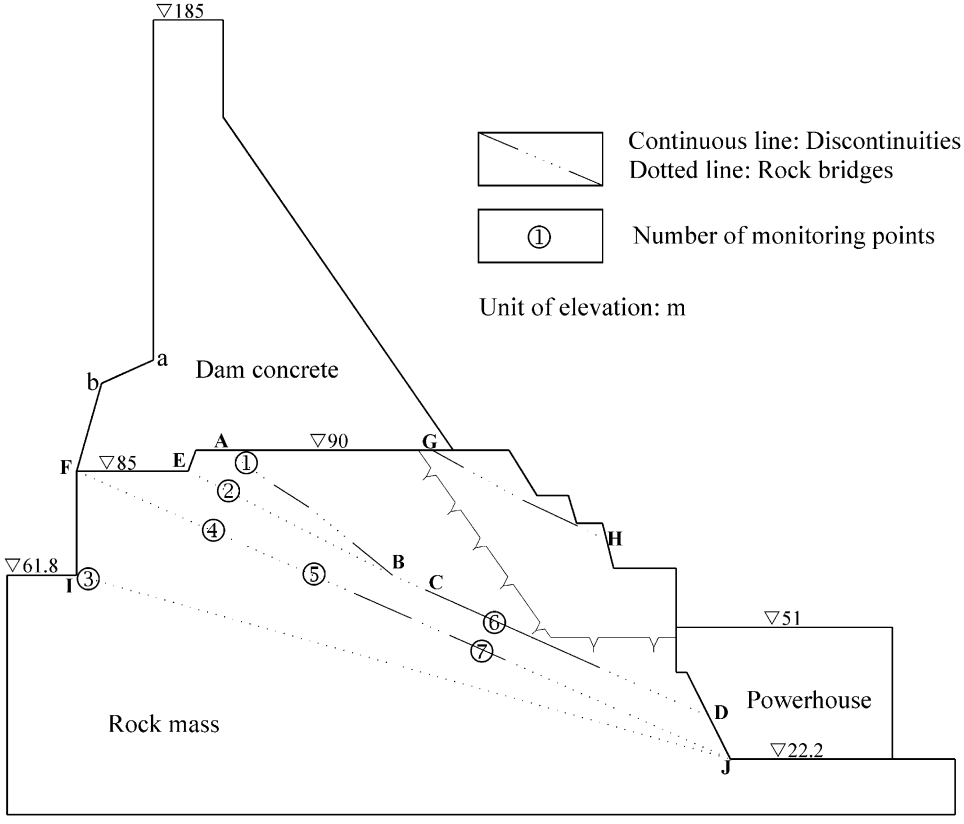

Fig. 14. Geological model of No. 2 left powerhouse-dam section of the Three-Gorges Dam.

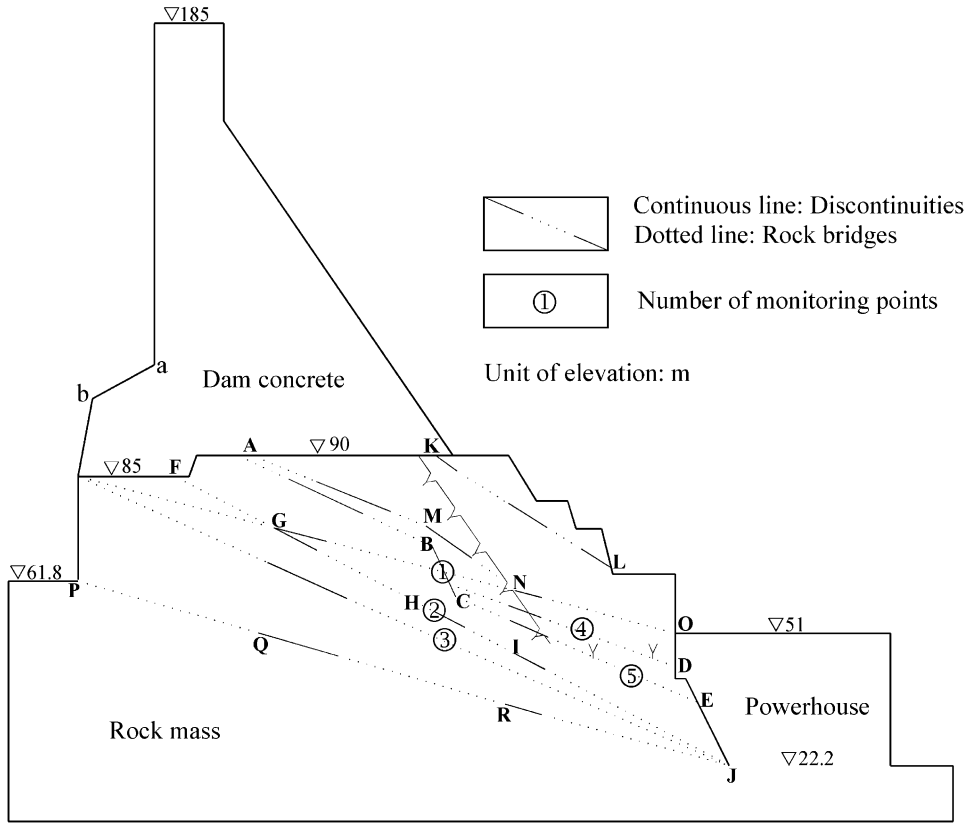

Fig. 15. Geological model of No. 4 left powerhouse-dam section of the Three-Gorges Dam.

Table 5
Characteristics of the main potential sliding paths in the geological model of no. 3 left powerhouse dam section (Refer to Fig. 13 for paths)

Potential sliding paths	Total length (m)	Length of long joints (m)	Length of rock bridges (m)	Length of short joints in rock bridges (m)	Ratio of length of joints to the total length (%)	Sections	Dip angles (°)
ABCDE	113.4	90	23.4	2.69	81.7	AB CDE	41 26
PBCDE	125.2	79.8	45.4	5.22	67.9	PBCDE	26
ABCDFGH	129.6	104.4	24.6	2.83	83.1	AB BCD DF FGH	41 26 52 32

Table 6
Characteristics of the main potential sliding paths in the geological model of no. 2 left powerhouse dam section

Potential sliding paths	Total length (m)	Length of long joints (m)	Length of rock bridges (m)	Length of short joints in rock bridges (m)	Ratio of length of joints to the total length (%)	Sections	Dip angles
ABC	124.4	41.0	83.4	9.59	40.7	AB BC	36° 21°
EBC	129.4	37.0	92.4	10.63	36.8	EB BC	27° 21°

Table 7
Characteristics of the main potential sliding paths in the geological model of no. 4 left powerhouse dam section

Potential sliding paths	Total length (m)	Length of long joints (m)	Length of rock bridges (m)	Length of short joints in rock bridges (m)	Ratio of length of joints to the total length (%)	Sections	Dip angles
ABCD	102.2	28	74.2	8.53	35.7	AC BC CD	23° 62° 19°
ABCE	109.4	28	81.4	9.36	34.2	AB BC CE	23° 62° 24°
FGH	140.6	28	112.6	12.95	29.1	FGH	26.5°

Table 8
Mechanical parameters of the foundation rock and joint plane used in the stability studies

Type	Compressive strength (MPa)	Density (kN/m^3)	Deformation moduli (GPa)	Poisson's ratio	Friction angle	Cohesion (MPa)
Plagioclase granite	100	27.0	35	0.20	59.6°	2.0
Joint planes	—	—	—	—	35°	0.2
Dam concrete	200	24.5	26	0.167	48°	3.0
Foundation surface	—	—	—	—	48°	1.3

Fumagalli systematically developed the theory and techniques of statical and geomechanical model tests, which had been applied to the stability assessment of a series of dams, such as Ridracoli, Itaipu, and Canelles, etc. [9,10,26]. Müller and Rossenblad studied the physical modeling methodologies of jointed rock mass [10,24]. Moreover, high-density and low-strength modeling materials for physical model test were also researched [27,28].

In this study, two physical model tests for no. 3 and no. 2–4 powerhouse-dam sections have been carried out. One is a 2D test considering only the no. 3 dam section and another is a 3D model considering three dam sections together, no. 2–4. The purpose of the latter is to examine the constraint effects of no. 2 and no. 4 sections on stability of no. 3 section. The similarity theory and experimental methods are described below.

4.1. Similarity theory

Physical models must satisfy a series of similarity requirements in terms of geometry, physical–mechanical properties, boundary conditions and initial states. According to elasto-plasticity theory and dimensional analyses, these similarity requirements can be deduced from force–equilibrium equations, geometry equations, Hooke's law and boundary conditions [9,10,26].

The theory requires that some similarity coefficients, defined as the ratios of prototype parameters to model parameters, must be constants. These prototype parameters are geometry, stress, strain, displacement, deformation modulus, Poisson's ratio, volume force, density, friction coefficient, cohesion force, compress strength and boundary stress, respectively [9,10,26]. Their similarity constants are defined as

$$C_L = L_p/L_m, \quad C_\sigma = \sigma_p/\sigma_m, \quad C_\varepsilon = \varepsilon_p/\varepsilon_m, \quad C_\delta = \delta_p/\delta_m, \tag{1a}$$

$$C_E = E_p/E_m, \quad C_\nu = \nu_p/\nu_m, \quad C_X = X_p/X_m, \quad C_\rho = \rho_p/\rho_m, \tag{1b}$$

$$C_f = f_p/f_m, \quad C_c = c_p/c_m, \quad C_R = R_p/R_m, \quad C_{\bar\sigma} = \bar\sigma_p/\bar\sigma_m, \tag{1c}$$

where C_L, C_σ, C_ε, C_δ, C_E, C_ν, C_X, C_ρ, C_f, C_c, C_R, $C_{\bar\sigma}$ represent the similarity constants for geometry, stress, strain, displacement, deformation modulus, Poisson's ratio, volume force, density, friction coefficient, cohesion force, compress strength and boundary stress, respectively. The symbols L, σ, ε, δ, E, ν, X, ρ, f, c, R, $\bar\sigma$ denote the parameters of geometry, stress, strain, displacement, deformation modulus, Poisson's ratio, volume force, density, friction coefficient, cohesion force, compress strength and boundary stress. The subscript p denotes that the corresponding parameter is of prototype, while the subscript m indicates that the corresponding parameter is that of the physical models.

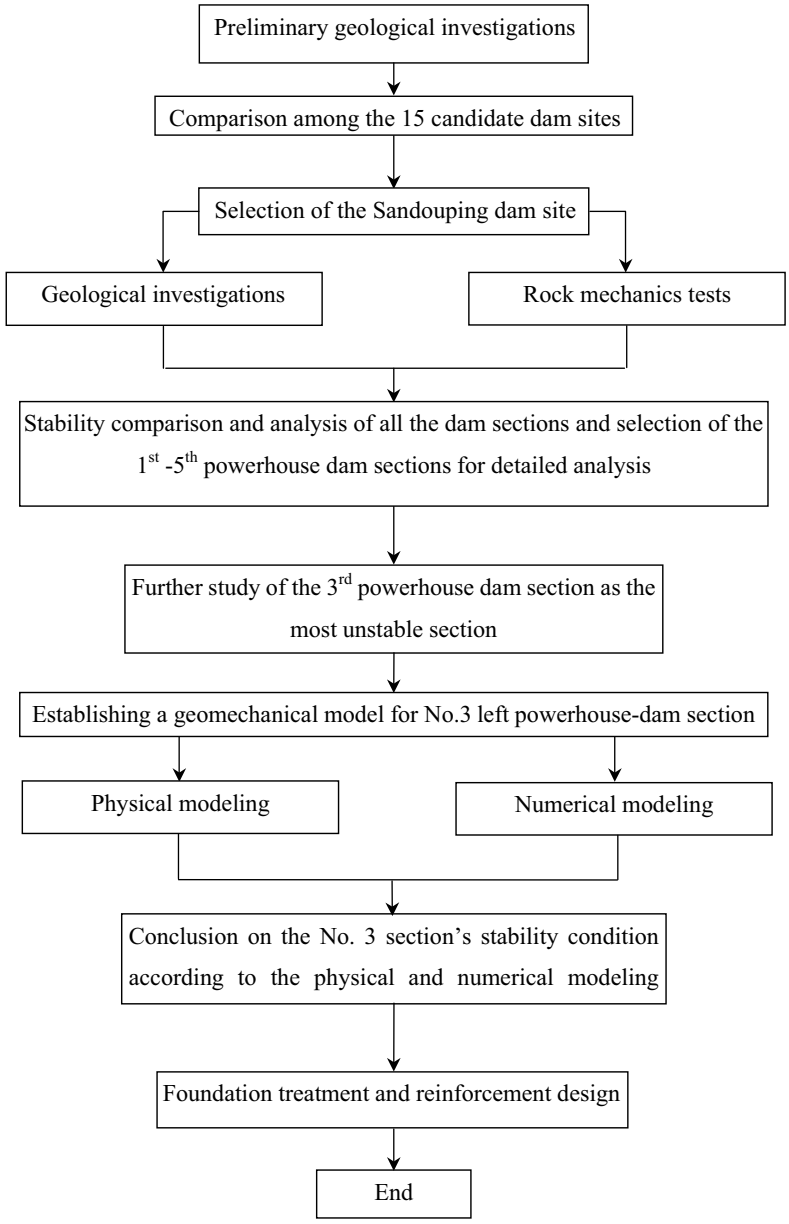

Fig. 16. Flowchart of the stability study procedure for the Three-Gorges Dam foundation.

The following similarity criteria must also be met in the physical modeling:

$$\frac{C_\sigma}{C_\rho C_L} = 1, \tag{2}$$

$$C_\varepsilon = C_\rho = 1, \tag{3}$$

$$\frac{C_\varepsilon}{C_\rho} = 1, \quad \frac{C_\delta}{C_L} = 1, \quad \frac{C_c}{C_\sigma} = 1, \quad \frac{C_\sigma}{C_R} = 1, \quad \frac{C_{\bar{\sigma}}}{C_\sigma} = 1, \tag{4}$$

$$C_f = 1. \tag{5}$$

These criteria are the guiding parameters for choosing or manufacturing the modeling materials of the physical model tests with specified mechanical properties, model size and proportions, magnitudes of loading forces, and boundary conditions [9,10,26].

4.2. Simulation of loads

Five kinds of loads were simulated in the physical modeling, including self-weight of dam and rock mass, water pressure, sediment pressure, and osmotic pressure acting on the grout curtain. From Eqs. (2) and (3), if C_ρ equals 1 and C_σ equals C_L, the self-weight stress regime of the model can satisfy the similarity requirements. Thus, the simulations of self-weights can be done by choosing the model materials that have the same densities as those of the corresponding prototype materials [9,10,26]. The water pressure,

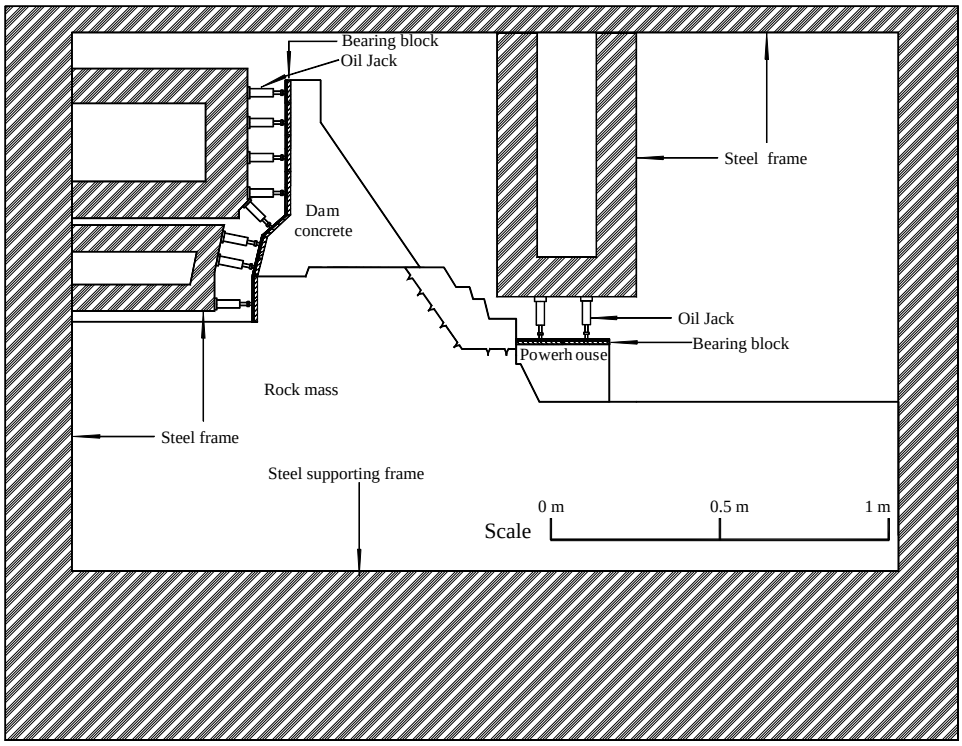

Fig. 17. Loading apparatus for the physical model tests.

sediment pressure and osmotic pressure acting on grout curtain were simulated by use of the loading system combined with oil jack, jacking block and jack-carrying steel frame (illustrated in Fig. 17) with their magnitudes satisfying both Eqs. (2) and (4). The seepage pressure in the dam foundation was not modeled in this study for the following reasons. On the one hand, the Three-Gorges Dam foundation mainly comprises plagioclase granite that is intact and of very low permeability; meanwhile, most of the joints in the foundation are not through-going and have a low connectivity with well-cemented tectonite, thus, the influence of seepage pressure on the stability of the dam foundation would not be so significant. On the other hand, to date, there are very few available data of the seepage pressure monitored from the dam foundation; besides, there is considerable difficulty in physical model tests to model the effects of seepage pressure [16,17,29,30].

In order to understand the failure mechanisms of the dam foundation, a progressive overloading that simulated the upstream hydrostatic water pressure was performed. The factor of safety was defined as the ratio between the maximum external load inducing the start of sliding instability of the dam foundation and the upstream hydrostatic load applied to the dam. The method of the overloading test was the so-called triangle overloading method through a progressive overloading of the upstream water pressure, which is assumed equivalent to the increase of water density; meanwhile, the self-weight of dam and rock mass remains unchanged. In the process of the modeling test, the upstream hydrostatic load was progressively applied according to the same increment steps until the dam fails. In each increment, 20% of the normal pool level (denoted as P_0) was applied.

4.3. Simulation of boundary conditions

The boundary conditions for both physical models were simulated in the same way: namely, the normal constraint was applied to the upstream and downstream boundaries (modeled by tight contacts between these boundaries and the rigid plate fixed in test frame), a fixed constraint to the bottom boundary (modeled by strong contact between these boundaries and the rigid plate fixed in test frame), and a free condition to the right and left boundaries of the models. Nevertheless, it should be noted that boundary conditions of the right and left boundaries of no. 3 dam section are different in these two physical model tests—which are free in the physical model of the single no. 3 section but are constrained by the adjacent foundations of no. 2 and no. 4 sections in the physical model of the integrated no. 2–4 sections.

4.4. Monitoring

In the physical modeling, the main objective of monitoring is to capture the displacements and their

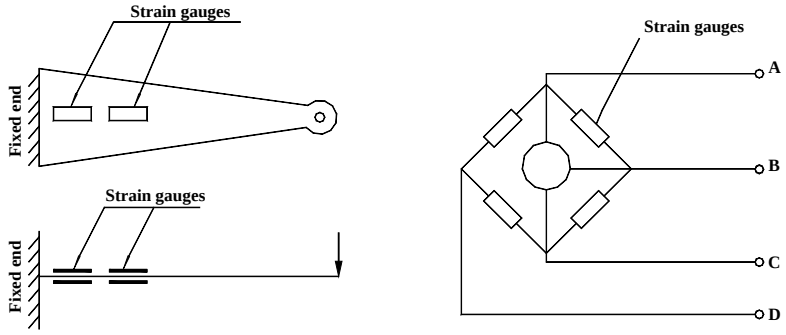

Fig. 18. Internal displacement sensor for the relative displacement monitoring adopted in the physical model tests.

Table 9
Similarity coefficients between prototype parameters and model parameters used for the 2D physical model test of no. 3 left powerhouse dam section

C_L	C_ρ	C_E	C_σ	C_c	C_f	C_ε
150	1.0	162	162	162	1	1

development processes so that we can identify the stability state of the dam. The displacements monitored in the models include absolute displacements (surface displacement of dam and foundation) and relative displacements (internal displacement between the upper and lower sides of the fractures). The former were measured by inductive displacement sensors with a precision of 0.001 mm, which was installed in a fixed steel frame made for this specific measuring objective. The latter were monitored by internal displacement sensors (strain-gauged cantilevers) with the same precision, which were buried in the lower side of the fracture, while a corresponding device was fixed in the upper side (Fig. 18). For the positions of monitoring points of relative displacements, see Figs. 13–15.

5. Physical modeling of no. 3 powerhouse-dam section

5.1. Similarity coefficients, simulation scope and model materials

Table 9 lists major similarity coefficients determined for this physical model tests. The dimensions of the dam foundation to be modeled are 150 m depth from foundation surface downward, 38.3 m of width (the same as the dam body), 95 m in length directed upstream from the dam heel and 345 m in length directed downstream from the dam toe. Based on the geometry similarity coefficient of 150, the actual physical model has dimensions of 1.63 m height, 0.26 m width, 0.63 m (upstream direction) and 2.3 m (downstream direction) lengths. Fig. 19 shows a photograph of the physical model of no. 3 powerhouse-dam section.

To find out if the model materials met the similarity requirements, different combinations of raw materials (including gypsum powder, barite powder, lithopone, cement, bentonite, machine oil, paraffin oil, water, etc.) were firstly analyzed to obtain some tentative prescriptions. Then, different mixture ratios of these ingredients were chosen for each specific prescription. The mixtures were stirred sufficiently and pressed in press molding machine to produce several sets of model material specimens, whose properties were tested in laboratory. Finally, based on the test results, two mixture ratios of gypsum powder, barite powder, lithopone, machine oil and water were selected for simulating the concrete and rock. The joint surfaces were simulated by the unglued interfaces between model material blocks (which are normally glued to construct the models). The shear strength of this model interface was tested. Table 10 lists the major properties of model materials, prototype materials and joint surfaces, showing an acceptable similarity in material properties between the model and prototype.

5.2. Modeling results and analyses

Table 11, Figs. 20 and 21 present the major displacement results and their development processes derived from the physical model test for the no. 3 dam section. The monitored displacements were converted into prototype displacement using the similarity coefficients. According to these results, three different stages of the displacement development can be identified, following the increases of the upstream hydrostatic loading.

A displacement development during the upstream hydrostatic load increases from zero to $1.8P_0$ can be identified as the first stage. As shown in Fig. 21, at this stage all the load–relative displacement curves along the potential sliding planes remain as straight oblique lines. This indicates that during this loading process, the dam foundation behaves elastically without sliding along any potential failure surfaces in the foundation. In addition, as shown in Table 11, under normal loading combination ($1.0P_0$), the magnitudes of the horizontal

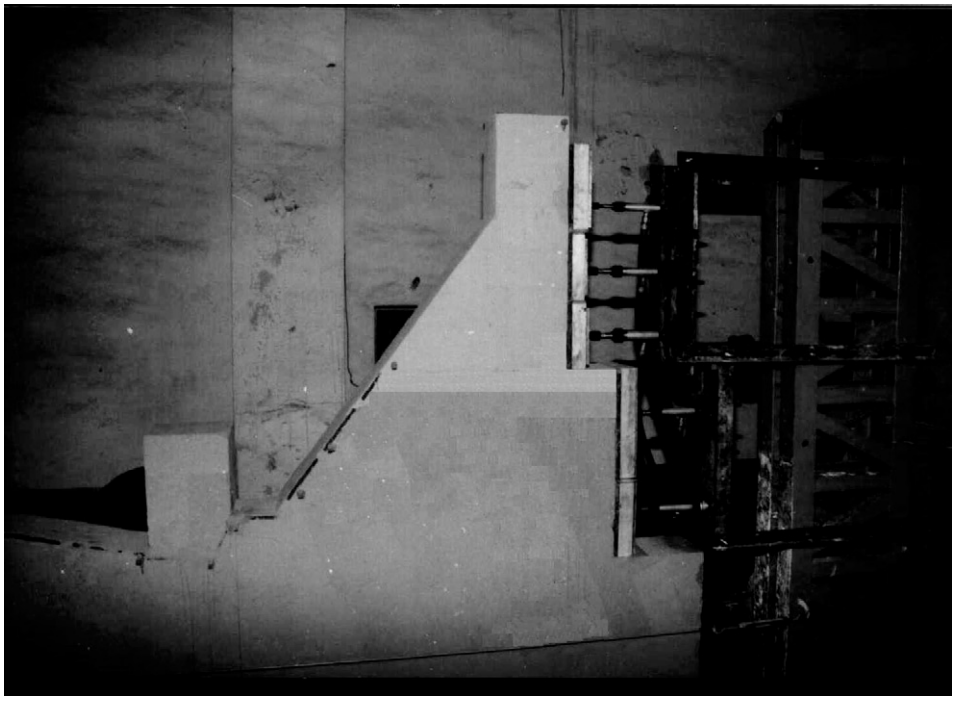

Fig. 19. The physical model of no. 3 powerhouse-dam section of the Three-Gorges Dam.

Table 10
Comparison of mechanical properties of 2D physical model materials and prototype materials of no. 3 left powerhouse dam section

Mechanical properties	Rock		Dam concrete		Joint		Foundation surface	
	Prototype	Model	Prototype	Model	Prototype	Model	Prototype	Model
Deformation modulus (GPa)	35.0	0.210	26.0	0.160	—	—	—	—
Density (kN/m^3)	27.0	25.0	24.5	22.7	—	—	—	—
Friction angle	59.6°	59.3°	48°	46°	35°	34.6°	48°	47.5°
Cohesion (MPa)	2.0	0.053	3.0	0.051	0.2	0.0	1.3	0.065

Table 11
Displacements of key positions of no. 3 left powerhouse dam section under normal loading combination monitored from the 2D physical model test

Displacements of dam top (mm)		Displacements of dam heel (mm)		Displacements of dam toe (mm)	
Horizontal	Vertical	Horizontal	Vertical	Horizontal	Vertical
14.85	3.30	2.10	1.13	2.10	−0.37

displacements at both dam heel and toe are 2.10 mm, indicating that the shear strength along the foundation surface is sufficient so that the horizontal displacements along this surface are small. Based on the above analyses, it can be concluded that the dam foundation is stable until $1.8P_0$; and, the safety of the dam can be ensured under normal loading combination.

A displacement development during the upstream hydrostatic load increases from $1.8P_0$ to $3.5P_0$ can be identified as the second stage. As shown in Fig. 21, after the upstream hydrostatic load was applied up to $1.8P_0$, the slopes of the load–relative displacement curves at points 1, 2, 4 and 6 (see Fig. 13 for the locations of these points) decreases gradually. Under the overloading of $1.8P_0$, the first turning points appear on these curves. This indicates that along the assumed slide planes of ABCD, IC and KNO (see Fig. 13), plastic shear deformations occurs, with the result that at these

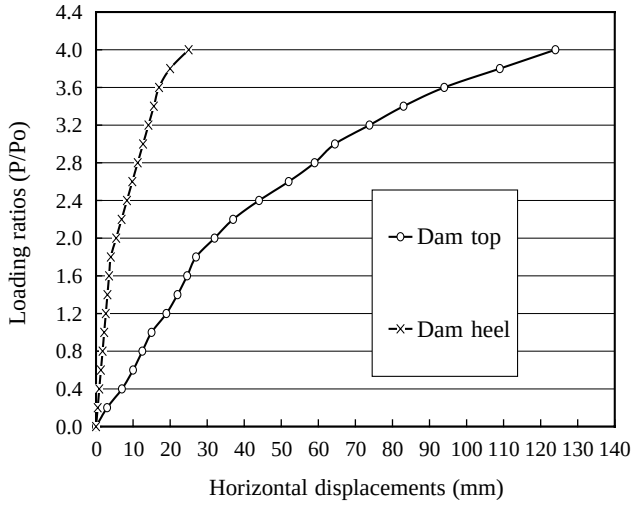

Fig. 20. Load-horizontal displacement curves of monitoring points of the no. 3 powerhouse-dam section derived from the 2D physical model test.

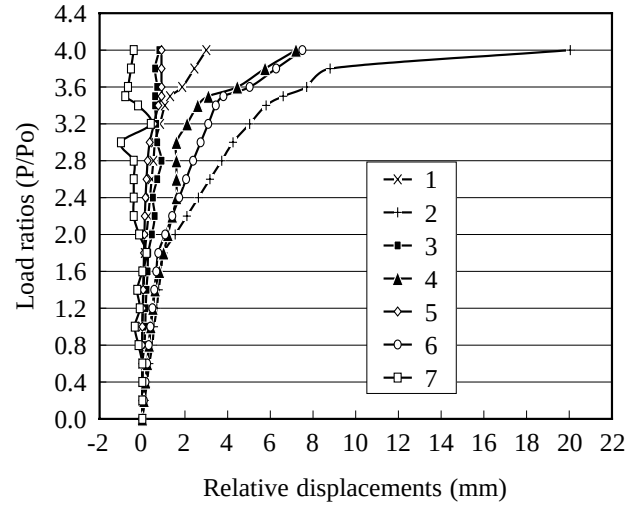

Fig. 21. Load–relative displacement curves of monitoring points of the no. 3 powerhouse-dam section derived from the 2D physical model test.

monitoring points, the rate of increase of the displacements is larger than before. Nevertheless, the dam remains stable at the second stage.

The third stage can be defined as the process from the loading of $3.5P_0$ until the dam failure. At this stage, the slopes of load–relative displacement curves at points 1, 2, 4 and 6 decrease dramatically, with abrupt increase of displacements and occurrence of second turning points on these curves. However, this situation does not occur at other monitoring points. The above results indicate that after the load application of $3.5P_0$, the sliding along the paths of ABCD, ICD and KNO (see Fig. 13) occurs simultaneously, and may cause dam failure. On the other hand, fracture traces (shown in Fig. 22) can be observed on the model surface along the above sliding paths, and along aA and bA paths (cf. Figs. 13 and 22) in the dam itself. This reveals that the concrete strength of the dam plays an important role in sliding resistance.

Depending on the above analyses, a conclusion can be drawn that the sliding starts under the overloading of $3.5P_0$. Thereby, if the factor of safety is defined as the ratio between the failure load and the normal hydrostatic load [5], it should be 3.5.

6. Physical modeling for no. 2–4 powerhouse-dam sections

6.1. Similarity coefficients, simulation scope and modeling materials

To study the constraint effects applied by the foundations of no. 2 and no. 4 dam sections on the stability of no. 3 dam section between them, a 3D physical modeling of the combined no. 2–4 dam sections was conducted.

Table 12 lists major similarity coefficients designed for this model. The dam foundation has the dimensions of 140 m depth, 114.9 m width (the same as the dam bodies), and 74 m in length directing upstream from the dam heel and 250 m in length directing downstream from the dam toe. According to a geometry similarity coefficient of 120, the actual physical model has the dimensions of 1.96 m height, 0.96 m width, 0.62 m (upstream direction) and 2.08 m (downstream direction) lengths. The model material ingredients were the same as those of the no. 3 dam section model, but different mixture ratios of these ingredients were used for simulating the rock and concrete for these two sections. The rock bridges and joints faces were simulated in the same way as the 2D model simulating the no. 3 dam section. The major properties of all the model materials were also tested and are listed in Table 13. It should be noted that in this model, the left and right boundaries of no. 3 dam section are, respectively, connected with the foundations of no. 2 and no. 4 sections, the latter would produce constraint effects on the foundation of no. 3 section. In addition, the left side of no. 2 section and the right side of no. 4 are treated as free surfaces.

6.2. Modeling results and analyses

Since the stability of the single no. 3 dam section had been studied first, for model tests of no. 2–4 dam sections, only one monitoring point was selected for the result analysis. This monitoring point positions at no. 1 point is shown in Fig. 13.

Similar to the model test of no. 3 dam section, three different stages of the displacement development can also be identified during the physical model test of the

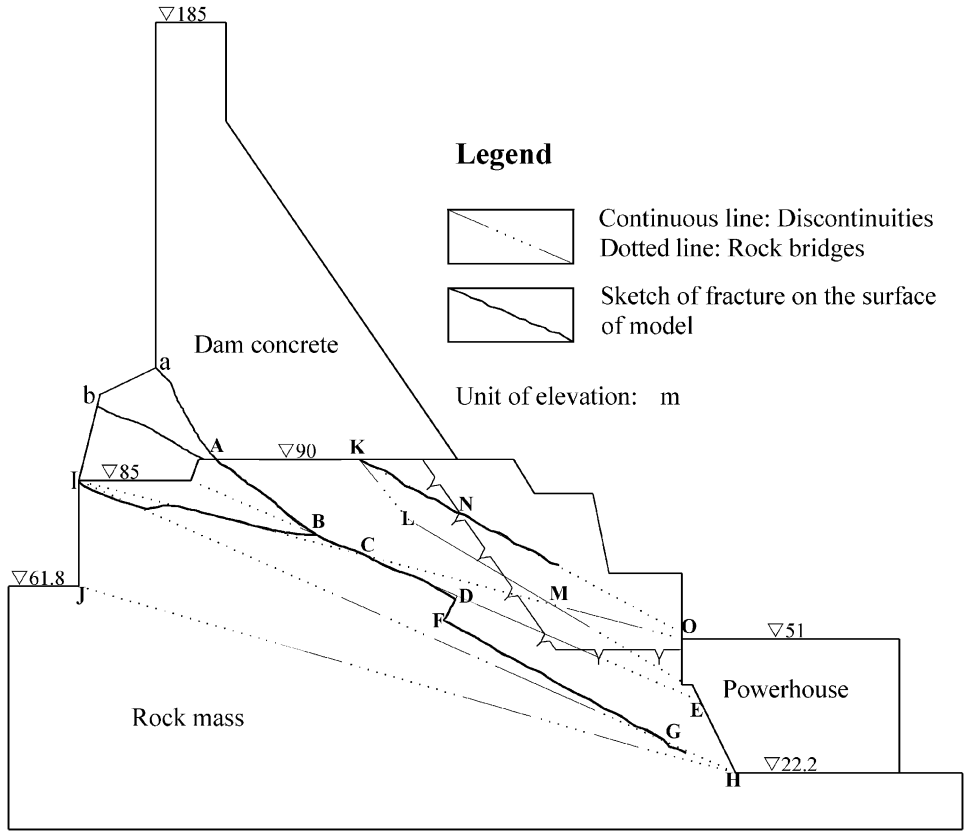

Fig. 22. Sketch of fracture traces on the model surface of the no. 3 powerhouse-dam section observed from the 2D physical model test.

Table 12
Similarity coefficients between prototype parameters and model parameters determined for the 3D physical model test of no. 2–4 left powerhouse dam sections

C_L	C_ρ	C_E	C_σ	C_c	C_f	C_ε
120	1.0	120	120	120	1	1

no. 2–4 dam sections (see Figs. 23–25). From zero to the normal loading combination ($1.0P_0$), all the load–relative displacement curves derived from this modeling appear to be straight oblique lines. This indicates that at this stage, the dam foundations behave elastically and sliding does not occur. As shown in Table 14, under the normal loading combination, the magnitudes of the horizontal displacements at both dam heel and toe of no. 3 dam section are less than 2.0 mm.

Fig. 23 reveals that under the load application of $4.0P_0$, the final turning point appears on the load–relative displacement curve at point 1. At this turning point, the slopes of this curve dramatically decreases and the relative displacement increases abruptly. This demonstrates that the sliding in the foundation of no. 3 dam section occurs at the overload of $4.0P_0$, when no. 2 and no. 4 dam sections' constraint effect was considered and thereby, the factor of safety of this dam section could be defined as 4.0.

From Fig. 24, we find that the load–relative displacement curves at no. 1, 2, 4, 6 and 7 have their respective final turning points under the overloading of $4.2P_0$, $4.4P_0$, $4.4P_0$, $4.4P_0$ and $4.8P_0$, respectively. These plots show that the sliding in the foundation of no. 2 dam section happens first along the slide path of ABCD, and then EBCD and FB (see Fig. 14). Simultaneously, the fracture traces (depicted in Fig. 26) along these slide paths and aA path in the dam itself were observed on the corresponding side faces of the model. Therefore, it further demonstrates that the shear strength of the dam plays a helpful role in the sliding resistance, and the factor of safety of no. 2 dam section could be defined as 4.2.

As for no. 4 dam section, the load–relative displacement curves at monitoring points 1–5 have their final turning points at the load of $4.2P_0$, $4.6P_0$, $4.4P_0$, $4.6P_0$ and $4.8P_0$ (as shown in Fig. 25), respectively. This is to say that the sliding in the foundation of this section follows along the paths of ABC, then CD, and finally CE (see Fig. 15). This failure mechanism of no. 4 section also was demonstrated by the observation of the fracture traces on the model surface (illustrated as Fig. 27). Based on this failure mechanism, the factor of safety of no. 4 dam section can be defined as 4.2.

Table 13
Comparison of mechanical properties of 3D physical model materials and prototype materials of no. 2–4 left powerhouse dam sections

Mechanical properties	Rock		Dam concrete		Joint		Foundation surface	
	Prototype	Model	Prototype	Model	Prototype	Model	Prototype	Model
Deformation modulus (GPa)	35.0	0.305	26.0	0.21	—	—	—	—
Density (kN/m^3)	27.0	26.8	24.5	24.6	—	—	—	—
Friction angle	59.6°	59.5°	48°	48°	35°	34.2°	48°	45°
Cohesion (MPa)	2.0	0.045	3.0	0.052	0.2	0.0	1.3	0.056

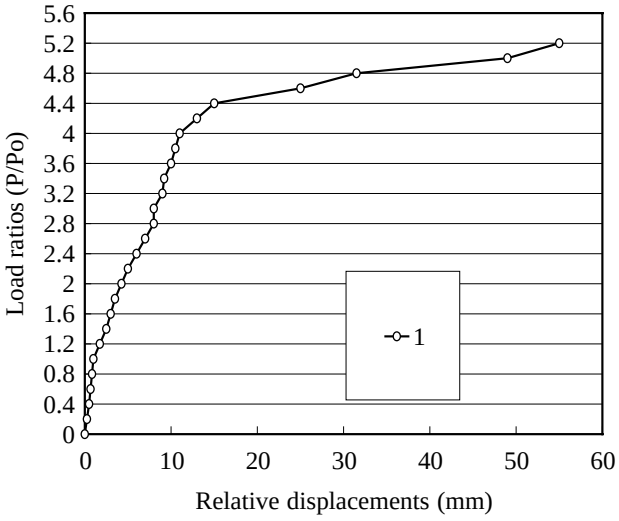

Fig. 23. Load–relative displacement curves of monitoring points of the no. 3 powerhouse-dam sections derived from the 3D physical model test.

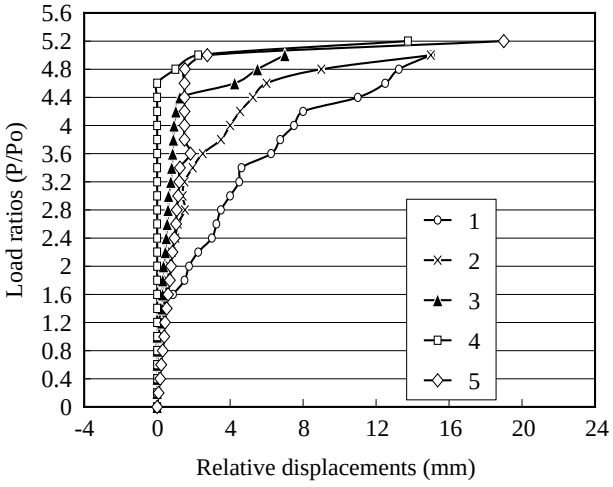

Fig. 25. Load–relative displacement curves of monitoring points of the no. 4 powerhouse-dam sections derived from the 3D physical model test.

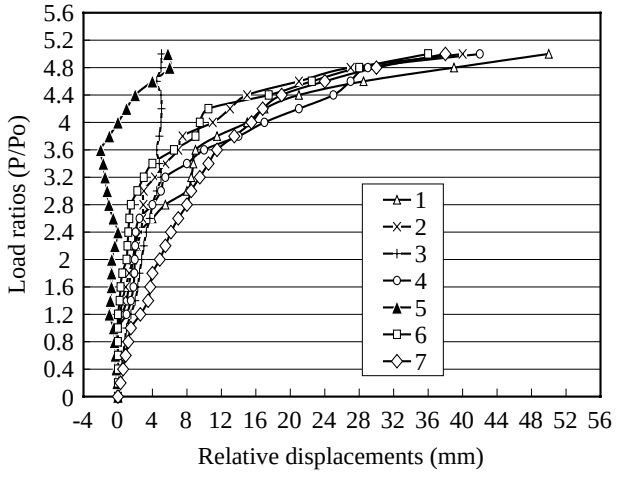

Fig. 24. Load–relative displacement curves of monitoring points of the no. 2 powerhouse-dam sections derived from the 3D physical model test.

7. Comparisons and discussions

Comparing the horizontal displacements at the dam top and toe of no. 3 dam section derived from the two physical model tests, it can be found that their magnitudes decrease from 14.85 (top) and 2.10 (toe) to 11.74 (top) and 1.20 mm (toe) (cf. Table 11 and Table 14), respectively. Consequently, the factor of safety of the no. 3 section increases from 3.5 (considering only no. 3 section) to 4.0 (considering constraint effects of no. 2 and no. 4 sections).

On the other hand, according to the results derived from the second model test, the factor of safety of no. 3 dam section, which is determined as 4.0, is lower than those of no. 2 and no. 4 section (both are 4.2). This agrees with the conclusion of the geological conceptualization that the foundation stability of no. 3 dam section is poorer than that of no. 2 and no. 4 dam section.

From this study, it has been found that physical model tests have the following advantages. Firstly, since the rock bridges can be simulated directly using the same methods as that of the foundation rock, it is a more convenient and straightforward approach in this regard. Secondly, in the physical model tests, the factor of safety is defined as the ratio between the maximum external load inducing the start of sliding instability of the dam foundation

Table 14
Displacements of key positions of no. 2–4 dam sections under normal loading combination monitored from the 3D physical model test

Dam sections	Displacements of dam top (mm)		Displacements of dam heel (mm)		Displacements of dam toe (mm)	
	Horizontal	Vertical	Horizontal	Vertical	Horizontal	Vertical
No. 2 section	11.42	2.67	1.96	1.02	1.08	−1.44
No. 3 section	11.74	2.1	1.85	0.95	1.20	−1.32
No. 4 section	10.48	3.0	2.55	0.51	1.02	−1.02

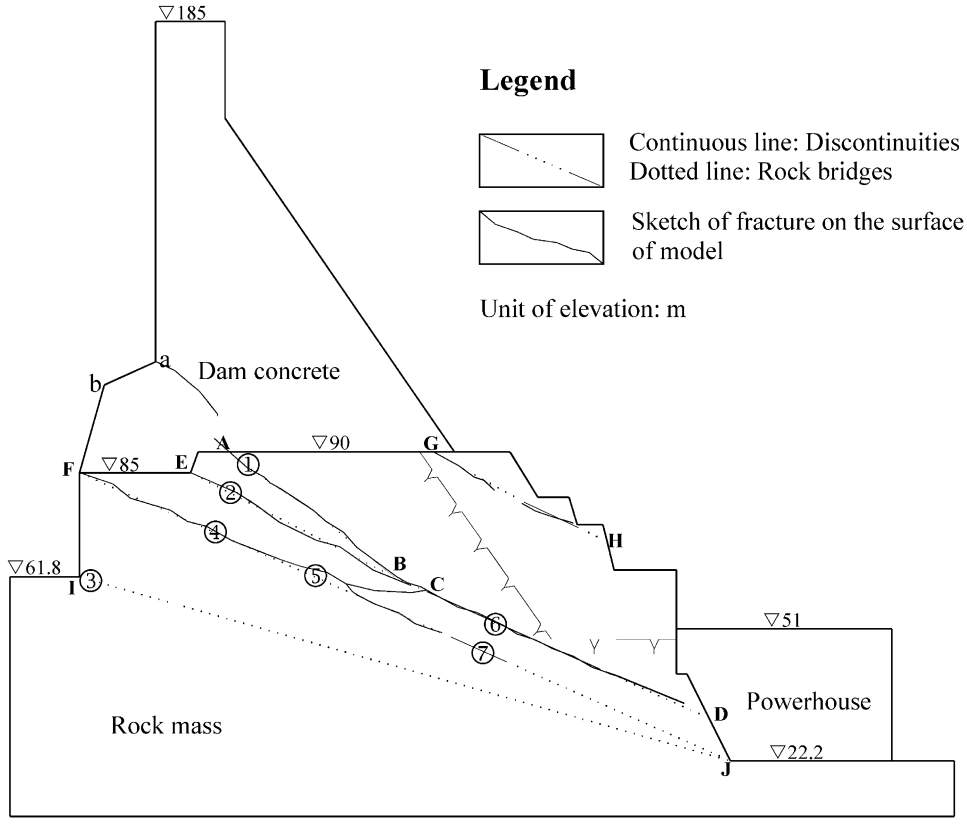

Fig. 26. Sketch of fracture traces on the model surface of the no. 2 powerhouse-dam section observed from the 3D physical model test.

and the upstream hydrostatic load applied to the dam. Therefore, it gives an indication of the foundation capability to withstand external loads. Moreover, by using the overload test, the physical modeling can reveal the most critical sliding mechanisms of potential dam failure.

In practice, the dam failure can be caused by other factors, namely the gradual decrease of the shear strength of joints due to seepage, deformation and damage, and geochemical reactions between water and fracture surface minerals. To date, it is difficult for the physical modeling techniques to consider such effects of the shear strength reduction of joints. In addition, in a case such as a dam, since the maximum hydrostatic loads are not particularly certain factors, the definition of factor of safety adopted in the physical model tests may not be complete or fully representative [5].

8. Conclusions

The complexity of geological conditions and variability of the rock mass properties resulted in difficulties for the stability study of the Three-Gorges Dam foundation. Therefore, the conceptualization of the geomechanical conditions and determination of the study procedures was essential, and integration of multiple analysis methods were considered to be more effective and reliable approaches. In this paper, as Part I of the study, the physical model tests and results were used to study the foundation stability of some critical dam sections in the Three-Gorges Dam. The following conclusions can be drawn.

(1) Analyses and conceptualization of geomechanical conditions of the Three-Gorges Dam foundation shows that the gently dipping joints are the most

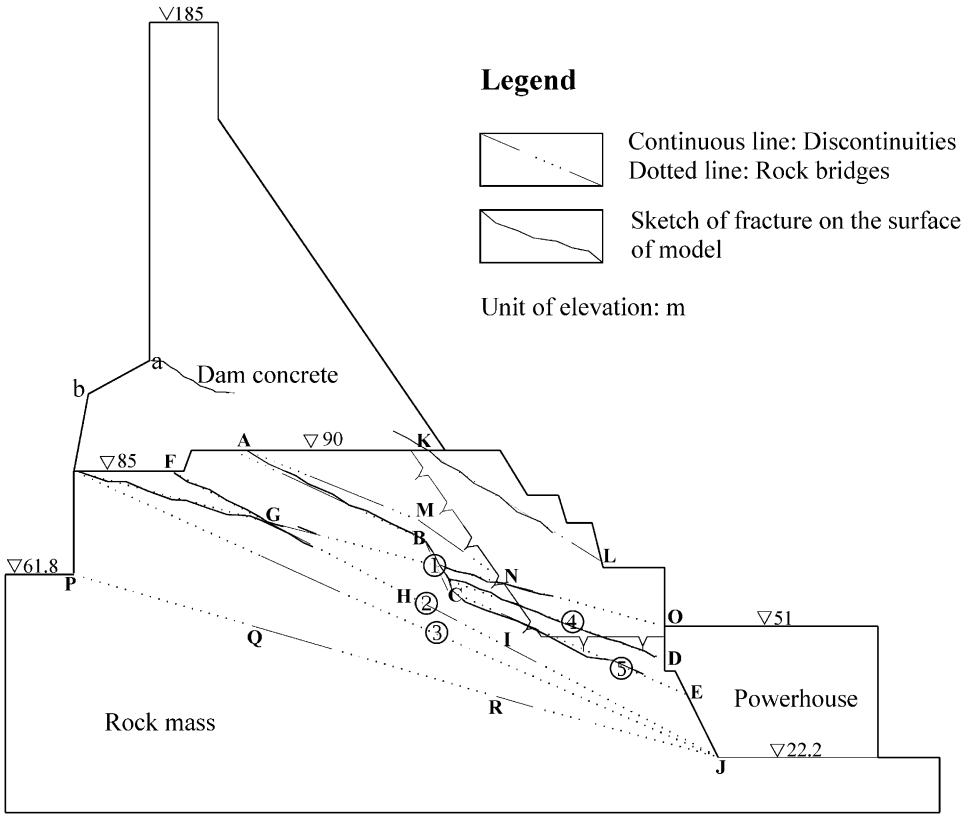

Fig. 27. Sketch of fracture traces on the model surface of the no. 4 powerhouse-dam section observed from the 3D physical model test.

important factors governing the foundation stability, and the foundation of no. 3 powerhouse-dam section is the most critical. This concept was verified by the results of the physical model tests.

(2) The results of the physical model tests show that under normal load combination, the foundation stability of no. 3 dam section is sufficient. The potential sliding and failure of this dam section could happen mainly along the potential sliding path of ABCDFGH (see Fig. 22).

(3) The physical model tests of the associated no. 2–4 dam sections demonstrated that the constraint effects induced by the adjacent foundations play a positive role in the foundation stability of the most critical no. 3 dam section, with the increase of its factor of safety from 3.5 (without considering constraints of no. 2 and no. 4 sections) to 4.0 (when their constraint effects were considered).

(4) Based on the Chinese Design Criterion for Concrete Gravity Dams (in which the factor of safety against sliding of concrete gravity dam must be more than 3.0), the experience from design and construction of many similar projects in China and the particular importance of the Three-Gorges Project, the Technical Committee of the Three-Gorges Project decided that the factor of safety against sliding of the Three-Gorges Dam must be more than 3.0 [16,17,19,31]. Hence, the results of the physical model tests indicate preliminarily that the stability of this dam section is ensured. Since the foundation of no. 3 powerhouse-dam section is the most critical in terms of stability against sliding failure, it can be tentatively deduced that the stability of the Three-Gorges Dam also satisfies the safety requirements.

Nevertheless, as stated previously in this paper, because of the incomplete definition of factor of safety adopted in the physical model tests and the unavoidable errors associated with the testing process, it is important to study and assess the stability of the Three-Gorges Dam foundation using other methods. For this reason, in Part II of this two part paper, numerical modeling, including FEM and LEM, are applied to analyze the stability of the Three-Gorges Dam foundation, based on the same geological conceptualizations and material properties. The purpose is mainly to study the effects of gradual degradation of fracture shear strength under normal loading combinations, which cannot be properly and effectively investigated by physical model tests.

Acknowledgements

The paper has been financial supported by the Three-Gorges Development Corporation, Changjiang Water Resources Commission, the Special Funds for Major

State Basic Research Project under Grant no. 2002CB412708, Pilot Project of Knowledge Innovation Program of Chinese Academy of Sciences under Grant no. KGCX2-SW-302-02, and National Natural Science Foundation of China under Grant no. 59939190. The inductive displacement sensors and model material pressing apparatus used in this study were provided by ISMES, Bergamo, Italy. The authors wish to thank all their colleagues in the Department of Structures and Materials, Yangtze River Scientific Research Institute, for their valuable contributions to various parts of the work described in the paper, particularly Professor Gong Zhaoxiong, Han Shihao, Shen Tai and Chen Jin, and Engineers Ye Liu, Sun Shaowen and Huang Mingxiao. The authors are also grateful to Dr. Lanru Jing, Royal Institute of Technology, Stockholm, Sweden, and Prof. J.A. Hudson for helping in preparing this paper.

References

[1] Chen DJ. Engineering geological problems in the Three-Gorges Project on the Yangtze China. Eng Geol 1999;51:183–93.
[2] MacLaughlin M, Sitar N, Doolin D, Abbot T. Investigation of slope-stability kinematics using discontinuous deformation analysis. Int J Rock Mech Min Sci 2001;38(5):513–37.
[3] Duncan JM. State of the art: limit equilibrium analysis and finite element analysis of slopes. J Geotech Eng, ASCE, 1996;122(7): 577–96.
[4] Shi GH. Discontinuous deformation analysis—a new numerical model for the static, dynamics of block system. PhD thesis, Department of Civil Engineering, University of California, Berkeley, 1988.
[5] Alonso E, Carol I, Delahaye C, Gens A, Prat P. Evaluation of factor of safety in discontinuous rock. Int J Rock Mech Min Sci Geomech Abstr, 1996;33(5):513–37.
[6] Jing L. Formulation of discontinuous deformation analysis (DDA)—an implicit discrete element model for block systems. Eng Geol, 1998;49:371–81.
[7] Ďurove J, Hatala J, Maras M, Hroncová, E. Support's design based on physical modeling. In: Proceedings of the International Conference of Geotechnical Engineering of Hard Soils–Soft Rocks. Rotterdam: Balkema, 1993.
[8] Wang C. The optimal support intensity for coal mine roadway tunnels in soft rocks. Int J Rock Mech Min Sci, 2000;37(7): 1155–60.
[9] Fumagalli E. Statical and geomechanical models. New York: Springer, Wien; 1973.
[10] Gong ZX, Liu J. Application and development of physical modeling techniques on the Three-Gorges Project. Beijing: Chinese Water Conservancy and Hydro-electric Power Publishers, 1996. p. 1–4 (in Chinese).
[11] Gong ZX. A discussion on the development trend of experimental mechanics. J Yangtze River Sci Res Inst, Wuhan, China, 1987; 4(1):10–3 (in Chinese).
[12] Liu J, Feng XT, Ding XL. Experimental and numerical analysis of foundation stability for no.3 powerhouse-dam section in the Three-Gorges Dam. In: Proceedings of the Fifth North American Rock Mechanics Symposium and the 17th Tunneling Association of Canada Conference, Toronto, Canada, 2002. p. 371–7.
[13] Liu J, Feng XT, Zhang J, Yue DM. Physical modeling on stability against sliding of left powerhouse dam of the Three-Gorges Dam. Chin J Rock Mech Eng 2002;21(7):993–8.
[14] Liu J, Ding XL. Study on the upstream lockhead foundation treatment of the shiplift of the Three-Gorges Project. Chin J Rock Mech Eng 2001;20(5):726–30.
[15] Ren ZM, Ma DX, Shen T, Tian Y. Study on rock engineering of the Three-Gorges Dam foundation. Wuhan: Chinese University of Geosciences Press, 1998. p. 253–300 (in Chinese).
[16] Yue DY, Jiang WQ, Liu JS. The comprehensive analysis of the stability against sliding of no. 1–no. 5 powerhouse dam sections of the Three-Gorges Dam. In: Research report by Yangtze Water Resources Commission, Wuhan, China, 1997 (in Chinese).
[17] Yue DY, Jiang WQ. The special design report of the foundation treatment of no. 1–no. 5 powerhouse dam sections of the Three-Gorges Dam. In: Research report by Yangtze Water Resources Commission, Wuhan, China, 1996 (in Chinese).
[18] Bao CG, Chen HK, Tian Y. Scientific research and experiment on the Three-Gorges Project. Wuhan: Hubei Science and Technology Press, 1997. p. 5–39 (in Chinese).
[19] Dong XC. Stability of the dam foundation, rock mass classification and optimization of the foundation line. In: Proceedings of the International workshop on Rock Engineering Related to the Three-Gorges Project, Yichang, China, 1993.
[20] Dong XC. Experimental study on rock mechanical properties at Sandouping dam site in the Three-Gorges Project. J Yangtze River Sci Res Inst, Wuhan, China, 1992;(suppl 1–10)A06;13–21 (in Chinese).
[21] Tian Y. Study on mechanical properties of rock mass of the Three-Gorges Project. J Yangtze River Sci Res Inst, Wuhan, China, 1992;(suppl 11–18)A06;72–76 (in Chinese).
[22] Li YL. Analysis, determination of mechanical parameters of the rock mass of the Three-Gorges Dam foundation. J Yangtze River Sci Res Inst, Wuhan, China, 1996;13(3):31–6 (in Chinese).
[23] Ding XL, Liu J, Liu XZ. Experimental study on creep behaviors of hard structural plane in TGP's permanent lock regions. J Yangtze River Sci Res Inst, Wuhan, China, 2000;17(4):30–3 (in Chinese).
[24] Müller L, Reik G, Fecker E, Sharma B. Importance of model studies on Geomechanics. In: Proceedings of the International Conference on Geomechanical model. Bergamo, Italy: ISRM, 1979.
[25] Alvarez MA. Mechanical models as compared with mathematics. In: Proceedings of the International Conference on Geomechanical model. Bergamo, Italy: ISRM, 1979.
[26] Fumagalli E. Geomechanical models of dam foundation. In: Proceedings of the International Colloquium on Physical Geomechanical models. Bergamo, Italy: ISRM, 1979.
[27] Barton NR. A low strength material for simulation of the mechanical properties of intact rock mechanics. In: Proceedings of the International Conference on Geomechanical model. Bergamo, Italy: ISRM, 1979.
[28] da silveira AF, Azeredo MC, Esteves Fereira MJ, Pereira da costa CA. High density and low strength materials for geomechanical models. In: Proceedings of the International Conference on Geomechanical model. Bergamo, Italy: ISRM, 1979.
[29] Liu J, Deng MY, Ye L. Physical modeling on the stability against sliding of no. 2–no. 4 left powerhouse dam sections of the Three-Gorges Project, China. In: Research report 97-036, Yangtze River Scientific Research Institute, Wuhan, China, 1997 (in Chinese).
[30] Liu J, Zhang J. Physical modeling on the stability against sliding of no. 3 left powerhouse dam sections of the Three-Gorges Project, China. Research report 96-281, Yangtze River Scientific Research Institute, Wuhan, China, 1996 (in Chinese).
[31] Ministry of Water Conservancy and Hydro-electric Power. DL5108-1999 Chinese Design Criterion of Concrete Gravity Dam. Beijing: Chinese Water Conservancy and Hydro-electric Power Publishers, 1999 (in Chinese).